Composite Patch Repair for Underwater Aluminum Structures

R. W. Bianchi
Department of Mechanical and Aerospace Engineering,
Naval Postgraduate School,
Monterey, CA 93943
e-mail: rwegele2011@gmail.com

Y. W. Kwon
Department of Mechanical and Aerospace Engineering,
Naval Postgraduate School,
Monterey, CA 93943
e-mail: ywkwon@nps.edu

E. S. Alley
Department of Mechanical and Aerospace Engineering,
Naval Postgraduate School,
Monterey, CA 93943
e-mail: esalley@nps.edu

Both experimental and numerical studies were conducted to investigate the effectiveness of composite patch repair on underwater structures, especially aluminum alloy structures. Physical samples were prepared using 5XXX aluminum plates with a premachined hole and E-glass woven fabric layers. The epoxy resin was selected such that it could be cured underwater. Test samples were prepared under different curing conditions such as dry curing and wet curing with different durations of in-water exposure. Strain gages were attached to all samples. The samples were tested for both tensile and four-point bending loads. Furthermore, numerical modeling and simulations were conducted, and the numerical models were validated against the experimental measurements. Then, the interface normal and shear stresses were determined from the numerical models so as to understand the delamination failure at the interface between the aluminum and composite patches. Underwater composite patching showed good interface strength and potential for successful usage in repairs.
[DOI: 10.1115/1.4042940]

Keywords: *composite patching, underwater application, aluminum alloy*

1 Introduction

Composite repair patching provides an alternative solution over other conventional repairs to metallic structures that are susceptible to stress corrosion cracking and fatigue cracking. Specifically, the structures, which are composed of aluminum alloy 5456, have been determined to be susceptible to cracking [1]. It was recognized that this aluminum alloy would become sensitized at higher temperatures resulting from the incorrect heat treatment processing received during the manufacturing process. Because of this sensitization, there have been many issues with cracking in the aluminum [1,2]. Sensitization refers to a harmful microstructure that increases the corrosion susceptibility in Al 5XXX series alloys. Sensitized aluminum alloy is observed in 5XXX alloys that have magnesium contents greater than 3% weight content and operate at temperatures reached by simple solar exposure [2].

Conventional repairs necessary in this "dry environment" include completely cutting out and removing the affected sections and conducting hot work (welding) repairs. In some situations, a weld repair cannot be performed, as called out in ASTM G67 which states a mass loss greater than 60 mg/cm^2 cannot be welded because cracks will form in the area adjacent to the weld repair [3]. These conventional repairs are time-consuming and costly.

The use of a carbon fiber reinforced composite patch was used as an alternative repair application. This technique was proved to be effective in many ship applications as a long-term temporary repair lasting at least 10 years in service [4]. A comparison of aluminum repair costs between composite repairs and weld repairs shows that the composite patch repairs are significantly lower than the weld repairs made.

Much research has been conducted for composite repair techniques [5–7]. The U.S. Navy has developed an approved procedure to repair the affected aluminum alloy area of concern and prevent crack growth while restoring the integrity of the compromised area utilizing composite patching [8]. The procedure currently does not recover the absolute structural integrity of the affected area but is used as a long-term repair. The repairs mentioned earlier were conducted for dry structures that are not in direct contact with water.

The underwater environment is harsh and unforgiving, especially to man-made systems. Offshore structures are subjected to severe environmental and operational conditions. These conditions, which consist of exposure to corrosion, external impacts, and exposure to operational stresses and fatigue loads, can cause minor and major damage to these structures. As a result, repairs are relatively frequent depending on the system, and they can range from underwater welding to utilizing cofferdams for dry repairs. These repairs have proven to be costly and time-consuming and in some instances have proven ineffective. Many different commercial activities have begun to explore the use of a water-activated resin and fiber-reinforced polymers of carbon or glass to conduct emergency repairs.

There are some successful examples of repairing corrosion damaged, stress fatigue damaged, and impact damaged systems in the underwater environment [9,10]. The examples are the Gandy Bridge and subsea pipeline repair. Unlike previous studies discussed with the application of composite repair patching above and below the water, this study is primarily concentrated with the feasibility of applying a composite repair patch directly to the damage in the underwater environment as a potentially faster and less costly repair. As previously stated, the current method for repair above water is placing a composite patch over the crack in order to redistribute the stress around the crack and through the composite. There is currently no method for repair of a hull crack for the underwater environment utilizing a composite patch. The application of a composite patch directly underwater is focused on providing divers the ability to execute a composite patch externally to the hull as a temporary repair to allow the ship to continue on its mission or return to port for more permanent repairs. This study investigated the effectiveness of underwater composite repairs on aluminum structures using both experimental and numerical techniques.

2 Experimental Procedure

Both tensile and four-point bending tests were undertaken to demonstrate the application of the bonded composite repair patch, to analyze the interface strength of the composite to the aluminum sample, and to capture the load carrying characteristics of the patch. The tensile test is useful for interface peeling failure while the bending test is useful for the interface shear failure. Both tests were conducted using a uniaxial testing machine. Figure 1 shows the testing configurations of both tensile and four-point bending tests. The tensile loading was applied at the loading rate of

---

Contributed by the Ocean, Offshore, and Arctic Engineering Division of ASME for publication in the JOURNAL OF OFFSHORE MECHANICS AND ARCTIC ENGINEERING. Manuscript received October 19, 2018; final manuscript received January 23, 2019; published online March 12, 2019. Assoc. Editor: Jonas W. Ringsberg.

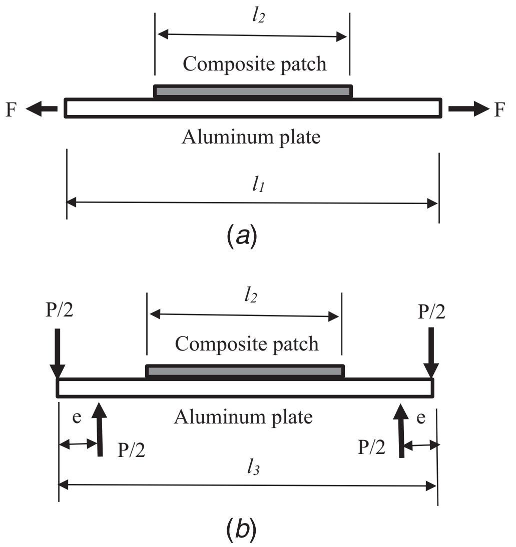

Fig. 1 Testing configurations: (*a*) tensile test and (*b*) four-point bending test with $l_1 = 0.26$ m, $l_2 = 0.15$ m, $l_3 = 0.17$ m, and e = 0.0215 m

F = 1 mm/min and the bending loading at the rate of P = 100 N/min to ensure the sample being tested under the quasi-static condition. The loading was continued until either failure of the test sample or reaching the maximum load programmed to the test.

The sample material to be patched is a 5052 H32 aluminum alloy. The predetermined defect size and shape chosen is in the form of a machined hole. It was decided to use a machined hole over a crack because a sharp crack is more difficult to generate consistently in test samples. The dimensions of the aluminum specimens and the holes used throughout this study are shown in Fig. 2 along with the corresponding dimensions listed in Table 1.

Composite patches were made of eight layers of 7500 Hexcel 6 ounce plain weave E-glass fabrics for composite patching. The composite was placed on the aluminum plate symmetrically from the centerline of the hole. A single layer of E-glass fabric was 0.15 m long, 0.1016 m wide, and 0.203 mm thick. The eight-layered composite patch was 1.94 mm including the resin material. The layer orientations were [(0/90)/(−45/45)/(0/90)/(−45/45)/(0/90)/(45/−45)/(90/0)/(45/−45)]. Because the composite was a woven fabric, (0/90) and (−45/45) denote one layer, respectively. The composite patch was quasi-isotropic.

For this study, Tyfo SW-1 Epoxy [11] was used for the resin and hardener to prepare the composite patches. The Tyfo SW-1 Epoxy is a two-part formulation consisting of part A (base) and part B (hardener). The SW-1 Epoxy is used in the underwater environment and should be mixed above water and then transported below water. Parts A and B are premixed individually and then combined in a clean container and mixed thoroughly. The mixing ratio is 100:74 by volume for the components A to B. The SW-1 Epoxy should be applied in water temperatures above 40 °F.

The lamination process for the wet patching consists of measuring and cutting dry fabric for the laminate stack, mixing the resin, and conducting the wet-out of the fabric directly onto the vacuum bag sheet, ensuring the stack is in line one on top of the other. Once the wet buildup is completed, the patch shall be handled by the vacuum bag sheet and brought into the tank for placement onto the submerged sample. Prior to beginning the patching procedure, the sample shall be prestaged onto the underwater workbench and held static via two C-clamps.

First, tensile tests were conducted for the standard aluminum samples without a hole as well as composite patch samples without attached to the aluminum, respectively, so as to determine their basic material properties. The aluminum samples showed their nominal material properties as shown in Table 1, while the composite patch was quasi-isotropic, the elastic modulus was 54 GPa, and Poisson's ratio was 0.16.

Then, tensile and four-point bending tests were conducted for samples prepared in different patching conditions, respectively. Each case was tested with two samples. The different test cases are described in Table 2. Four uniaxial strain gauges were attached to each specimen in order to measure the longitudinal strain at various locations of the samples as shown in Fig. 3. The placement of these strain gauges was chosen to ensure the region around the hole would be properly captured as load increases during the testing. During all tests, the applied load and strain gage readings were recorded.

3 Numerical Analysis

A series of finite element analyses (FEA) were conducted using ANSYS [12] to compare the numerical results with the experimental

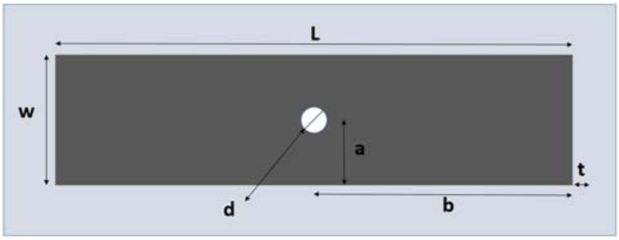

Fig. 2 Aluminum sample design with a machined hole

Table 1 Aluminum sample dimensions and material properties

Thickness (t)	2.032 mm
Width (w)	0.1016 m
Length (L)	0.3048 m
Hole diameter (d)	12.7 mm
Hole vertical offset (a)	0.508 m
Hole horizontal offset (b)	0.1524 m
Ultimate strength	228 MPa
Yield strength	180 MPa
Modulus of elasticity	74.3 GPa
Tangent modulus	500 MPa

Table 2 Test samples description

Sample designation	Description
A and B	Two samples with a machined hole and no patch (baseline testing).
C and D	Two samples with a machined hole and a composite repair patch conducted above the water and allowed to cure in the dry environment.
E and F	Two samples with a machined hole and a composite repair patch prepared above the water, applied to a submerged aluminum sample, and allowed to cure in the 3.5% NaCl water solution for 24 h.
G and H	Two samples with a machined hole and a composite repair patch prepared above the water, applied to a submerged aluminum sample, and allowed to cure in the 3.5% NaCl water solution for 1 week.
I and J	Two samples with a machined hole and a composite repair patch prepared above the water, applied to a submerged aluminum sample, and allowed to cure in the 3.5% NaCl water solution for 2 weeks.
K and L	Two samples with machined hole and a composite repair patch prepared above the water, applied to a submerged aluminum sample, and allowed to cure in the 3.5% NaCl water solution for 4 weeks.

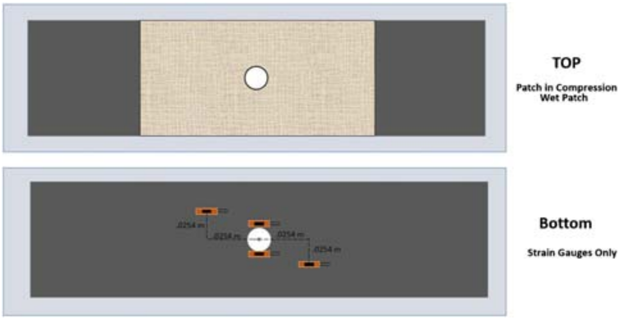

Fig. 3 Strain gage locations for the tensile and bending tests

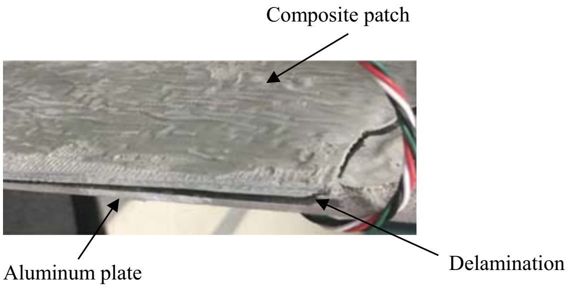

Fig. 4 A sample showing delamination between the aluminum and patch

data. More importantly, the numerical study was undertaken to find stresses at the interface between the composite patches and aluminum plates because no direct measurement was available.

The computer models simulated both tensile and four-point bending loadings as depicted in Fig. 1, respectively. The aluminum plate was modeled as an elastic-plastic material with linear straining hardening while the composite patch was modeled as a linear elastic isotropic material using the material properties discussed in Sec. 2. The boundary and loading conditions were applied to the models as shown in Fig. 1. Tensile or bending loads were applied incrementally for static analyses.

The aluminum plate and the composite patch were modeled using three-dimensional eight-node solid elements. The composite patch was modeled as a smeared composite material instead of being modeled layer-by-layer because all the failure occurred at the interface between the aluminum and composite interface as shown in Fig. 4. The finite element mesh of the patched aluminum plate is shown in Fig. 5. The mesh was more or less uniform throughout the aluminum and composite models with a typical element size of 1 mm on their surfaces, and two elements were used through the thickness of the aluminum and patch composite, respectively, in order to represent the bending mode of the deformation.

To validate the computer models with the used FEA meshes, the stress concentration factors were compared between the FEA results without patch and the analytical solutions while the samples were within elastic deformations. The stress concentration factors were 2.40 and 1.70, respectively, for the tensile and bending loads from the FEA results. The analytical values were 2.60 and 1.70, respectively. Furthermore, the strains from the FEA results were also compared with the experimental data for each given load as shown later. The comparisons were good.

For the patched model, the average interface stress was computed near the edge of the aluminum-patch interface. Both peeling normal stress and shear stress were obtained, respectively. These interface stresses were used to determine the interface failure strength of the samples during the experiments. In other words, interface stresses were computed using FEA for the known failure load from an experiment. The tensile loading showed that the normal stress was much greater than the shear stress at the interface while the bending load showed the opposite. As a result, from both loadings, it was possible to find the critical shear and normal strength at the interface, respectively.

4 Results and Discussion

Because two samples out of the same group behaved consistently, one of the two samples was selected to represent the group in the following discussion. Figure 6 compares the strain versus load curves for samples A, C, and E. The strain was measured at the edge of each hole in the aluminum plate. As seen in the figure, the samples with a patch had a significant decrease in the strain over the same loading conditions. The load to reach yielding at the hole also increased with a patch. Sample A, the no patch case,

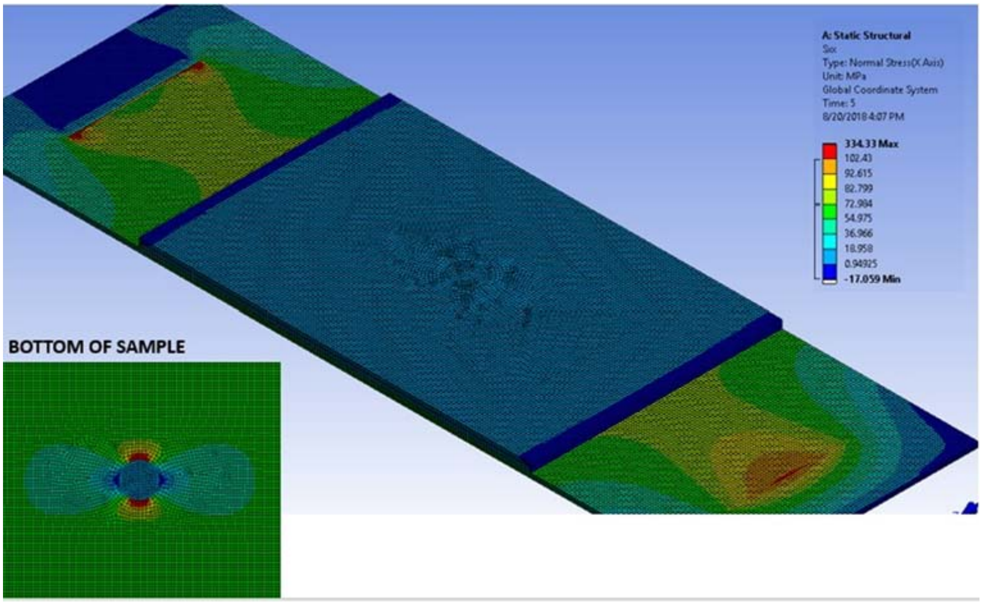

Fig. 5 Finite element mesh for patched specimen

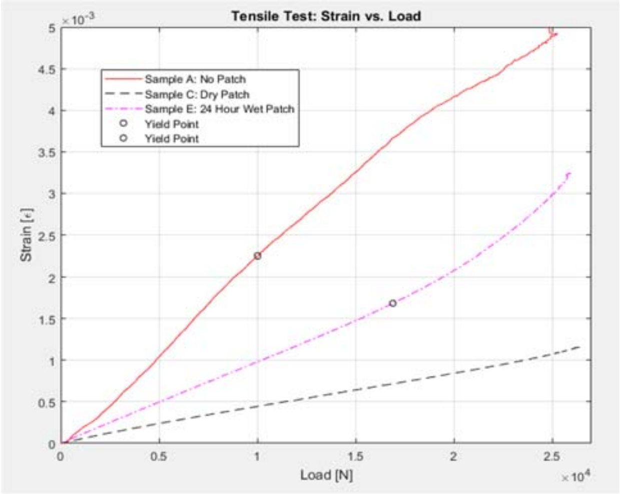

Fig. 6 Plots of load-strain for no patch, dry patch, and wet patch samples

reaches its yield point at approximately 10,000 N, whereas Sample E, the 24 h wet patch, reaches its yield point 16,900 N.

The samples that were patched in the underwater environment and left in to cure for a variable amount of time are the samples E–L. One sample from each time period is shown in a comparative graph of strain versus load as shown in Fig. 7. As seen in the figure, the samples that have been patched underwater and allowed to cure in the water for different amounts of time perform very similar in the tensile test. There were two samples that experienced failure in the mode of delamination. These points are displayed by star symbols in Fig. 7.

Analyzing the numerical results from the FEA of each patched sample tested under tensile loading, the normal (i.e., peeling) stress at the interface was significantly higher than the shear stress at the interface. These two stresses are the main contributors to the failure of delamination. Table 3 lists the peeling stress for each patched sample. For all samples that did not have delamination in the experiment, the peeling stress is shown at the patch interface for the maximum loading condition. For samples I and K that failed due to delamination under tensile loading, the peeling stress is shown at the patch/aluminum interface for the load at which the delamination occurred. The results showed that the two failed samples had a large variation in their failure strength. On the other hand, three other samples did not fail even though the shear stresses were close to or exceeded the failure stress in the other samples.

Table 3 Interface normal (peeling) stress under tensile loading

Sample	Load (kN)	Stress (MPa)
C: dry patch	26.11 (no failure)	8.87
E: 24 h wet patch	25.27 (no failure)	9.70
H: 1 week wet patch	25.71 (no failure)	9.71
I: 2 weeks wet patch	24.74 (delaimnation)	9.04
K: 4 weeks wet patch	12.05 (delamination)	4.69

Axial strains at the hole were compared between the numerical and experimental results for samples I and K at the loading condition of delamination. The percentage difference was about 5% and 7% for both specimens. The FEA model is considered to accurately represent the strain in the aluminum sample with the composite patch repair. The numerical peeling stress values acquired from the FEA are considered reliable based on the validation of the model.

Next experiments consisted of conducting four-point bending tests on 12 different samples. Since a fibrous composite is weaker under compression than tension, the four-point bending test was conducted such that the composite patch would be in compression for the conservative results.

Figure 8 compares the load versus strain curves for the first three categories of samples: no patch, dry patch, and 24 h wet patch samples. Examining the test results suggests that a composite repair patch applied to an underwater structure can significantly improve the structural integrity. The strain experienced at the hole, which is directly related to stress, is significantly decreased when a repair patch is applied. The solid line in Fig. 8 is Sample A, with no repair patch applied. This aluminum sample reaches its yield point at 470 N and begins to enter the plastic region. Sample C, the sample with a dry repair patch, did not reach a yield point, but failure mode of delamination occurred at 1070 N. Sample E, the sample with a wet repair patch, did reach neither a yield point nor delamination of patch until the predetermined applied load was reached.

One of the concerns with the application of a composite repair patch is the patch failing by delamination. The interface strength, or bonding strength, is a function of both shear stress and the normal (peeling) stress at the interface. Both stresses contribute to the delamination failure. However, if one stress is much larger than the other, the larger one will be the dominant stress causing the delamination. Both stresses were computed for all samples using the numerical data from the FEA models. In all cases, the shear stress was much larger out of the two. The shear stress

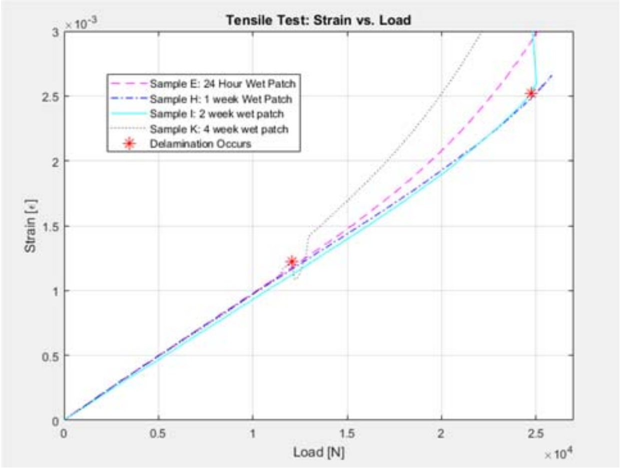

Fig. 7 Comparison of load-strain plots among wet patched samples with a variable amount of curing time in water

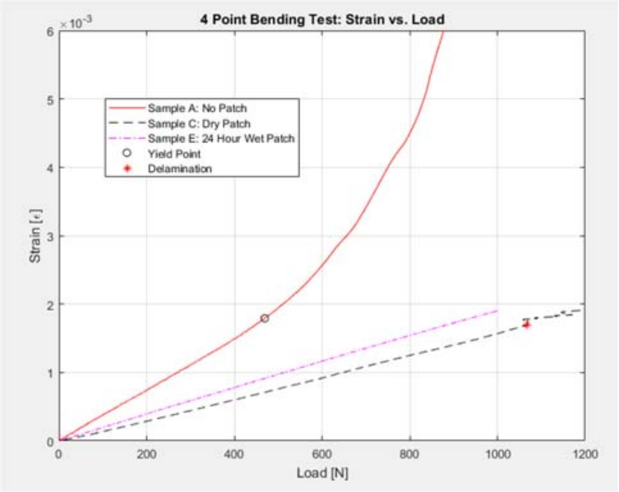

Fig. 8 Load-strain curve for Samples A, C, and E under bending load

Table 4 Interface shear stress under bending loading

Sample	Load (kN)	Stress (kPa)
C: dry patch	1.07 (delamination)	102.0
E: 24 h wet patch	1.02 (no failure)	102.2
H: 1 week wet patch	0.94 (no failure)	102.2
I: 2 weeks wet patch	1.48 (no failure)	54.4
K: 4 weeks wet patch	1.16 (delamination)	40.9

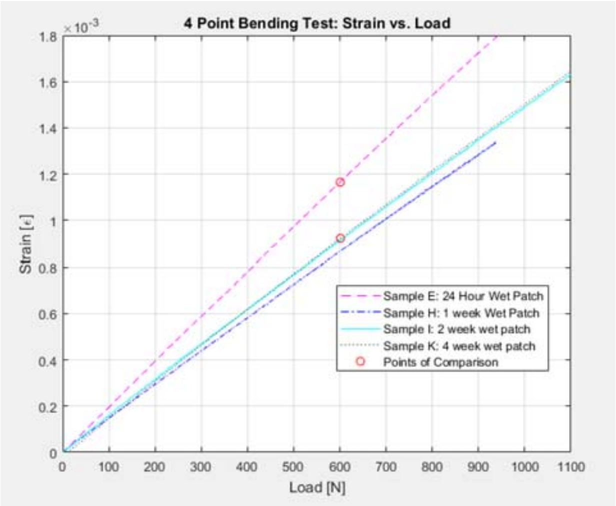

Fig. 9 Comparison of load-strain curves for wet patched samples under bending loads

Table 5 Comparison of experimental and numerical strains near the hole under bending loads

Sample	Load (N)	Experimental microstrain	FEA microstrain
A	380	1.048	1.170
C	540	0.824	0.725
E	540	1.048	0.981
H	540	0.782	0.919
I	540	0.935	0.823
K	540	0.766	0.850

at the maximum loading condition for all samples is shown in Table 4.

Samples E and H have a similar shear stress when compared with sample C, but the experiment showed no failure due to delamination. This has shown that the interface strength between the patch and the aluminum sample is stronger when the patch is left in the water to cure. All samples that were patched in the water are compared in Fig. 9. This graph shows that except for Sample E, all other samples have very close load-strain curves. In order to validate the computer models under bending loads, the experimental and numerical strains near the hole were compared at the given loads. Table 5 summarizes the comparison. Overall, the comparison was reasonable to support the numerical model.

During the testing, water absorption of this specific composite repair patch was investigated. An aluminum sample was patched using the dry repair patch procedure described earlier. This sample was immediately weighed and then placed in the underwater experimental tank. The sample was taken out of the water and weighed at 24 h, 1 week, 2 weeks, and 4 weeks interval. The results of the water absorption characteristics are summarized in Table 6. As shown, the composite repair patch had a 1.72% increase in mass after 168 h (1 week) spent in the water. Any time spent in the water after 168 h showed no further water absorption.

Table 6 Water absorption of composite repair patch

Time spent in water (h)	Mass (kg)
0	0.231
24	0.233
168	0.235
336	0.235
672	0.235

5 Conclusions

The overall goal of this study was to provide initial testing data to support that a composite repair patch can be effectively employed in the underwater environment to a damaged aluminum structure. Experiments were conducted to test the durability and effectiveness of the patch in two separate loading conditions: four-point bending loading and tensile loading. For each loading condition, patched samples were compared as they were prepared under different repair conditions such as dry and wet repairs.

The most important value assessed and used as a comparison for effectiveness of the patch was the strain in the aluminum measured near the hole. In both experiments and for all samples, the strain at the hole was measured and used to identify if the composite repair patch provided adequate reinforcement to reduce the strain in the aluminum samples. The underwater repaired samples did provide adequate reinforcement and the strain measured at the hole significantly lower than the sample without the patch. From a design failure standpoint, the numerical model of the FEA was used to assess the shear stress and peeling stresses at the interface of the patch to identify what was the dominant stresses during delamination. It was shown that the shear stress was the dominant stress for delamination failure for bending loads while the normal peeling stress was the dominant stress for tensile loads. For both experiments, it was proven that the interface strength between the patch and the aluminum surface was increased as the patch was allowed to cure in the water longer. This is an indication that in a combined loading condition, the patch would prove to be effective as well. The conclusion is that the underwater composite repair patch satisfied the research objective and that it is possible to repair underwater aluminum structures using a composite patch.

References

[1] Needham, B., and Field, A., 2007, *Sensitization of 5000 Series Al Alloys*, Naval Surface Warefare Center Carderock Division, Corrosion and Engineering Branch, Mega Rust Report, San Diego, CA.

[2] Schwarting, R., Ebel, G., and Dorsch, T., 2011, “Manufacturing Techniques and Process Challenges With CG47 Class Ship Aluminum Superstructures Modernization and Repairs,” Fleet Maintenance and Modernization Symposium 2001: Assessing Current and Future maintenance Strategies, San Diego, CA.

[3] ASTM, 2013, *ASTM G67-13; Standard Test Method for Determining the Suceptibility to intergranular Corrosion of 5XXX Series Aluminum Alloys by Mass Loss after Exposure to Nitric Acid (NAMLT Test)*, ASTM International, West Conhohocken, PA.

[4] Allan, R. C., 1983, “Carbon Fibre Reinforcement of Weld Repairs to the Aluminium Alloy Superstrucre of HMS Active,” AMTE(S) TM83475.

[5] Kwon, Y. W., and Hall, B. L., 2015, “Analyses of Cracks in Thick Stiffened Plates Repaired With Single-Sided Composite Patch,” Compos. Struct., **119**, pp. 727–737.

[6] Kwon, Y. W., Lee, W. Y., McGee, A. S., Hart, D. C., Loup, D. C., and Rasmussen, E. A., 2013, “Analytical Model for Prediction of Reduced Strain Energy Release Rate of Single-Side-Patched Plates,” Appl. Compos. Mater., **20**(6), pp. 1321–1339.

[7] Olson, T. M., Kwon, Y. W., Hart, D. C., Loup, D. C., and Rasmussen, E. A., 2015, “Carbon Nanotube Based Sensor to Monitor Crack Growth in Cracked Aluminum Structures Underneath Composite Patching,” Appl. Compos. Mater., **22**(5), pp. 457–473.

[8] Hart, D. C., 2017, "5xxx Aluminum Sensitization and Application of Laminated Composite Patch Repairs," Joining Technologies for Composites and Dissimilar Materials, Vol. 10, G. Cloud, E. Patterson, and D. Backman, eds, Conference Proceedings of the Society for Experimental Mechanics Series, Society for Experimental Mechanics, Indianapolis, IN.

[9] Suh, K. S., Mullins, G., Sen, R., and Winters, D., 2005, *Use of FRP for Corrosion Mitigation Applications in a Marine Environment*, Final Report for Florida Department of Transportation, Tallahassee, FL, October.

[10] Popineau, D., and Wiet, P., 2012, "Subsea Pipeline Repair by Composite System," Abu Dhabi International Petroleum Exhibition and Conference Society of Petroleum Engineers, Abu Dhabi, UAE, SPE-162509-MS.

[11] Tyfo SW-1, 2012, "FYFE Co., LLC," available: http://www.fyfeco.com/ Accessed: October 2, 2018.

[12] Kohnke, P., ed., 1994, *ANSYS Theory Reference*, Release 5.6, ANSYS, Inc., Canonsburg, PA.